Molecular Immunology 107 (2019) 10–20

Contents lists available at ScienceDirect

Molecular Immunology

journal homepage: www.elsevier.com/locate/molimm

Calreticulin induced endothelial ICAM-1 up-regulation associated with tristetraprolin expression alteration through PI3K/Akt/eNOS/p38 MAPK signaling pathway in rheumatoid arthritis

Yixin Liu[a,1], Wei Wei[b,1], Chengcheng Hong[c], Yang Wang[a], Xuguo Sun[a], Jun Ma[d,**], Fang Zheng[a,*]

[a] Department of Clinical Immunology, School of Medical Laboratory, Tianjin Medical University, Tianjin 300203, China
[b] Department of Rheumatology, General Hospital, Tianjin Medical University, Tianjin 300052, China
[c] Department of Laboratory Medicine, Children's Hospital of Tianjin, Tianjin 300203, China
[d] Department of Health Statistics, College of Public Health, Tianjin Medical University, Tianjin 300070, China

ARTICLE INFO

Keywords:
Calreticulin
Intercellular adhesion molecule-1
Signaling pathway
Tristetraprolin
Rheumatoid arthritis

ABSTRACT

The present study was undertaken to determine whether extracellular calreticulin (CRT) participates in the regulation of ICAM-1in rheumatoid arthritis (RA) and further explore the potential mechanism. Our results showed that ICAM-1 and VCAM-1 levels were positively correlated with CRT levels in RA serum and synovial fluid, respectively. In RA synovial tissue, increased co-expressions of CRT and ICAM-1 in vascular endothelium and perivascular areas and elevated co-location of CRT and VCAM-1 localized predominantly to lining layer were observed compared to those in OA. In in vitro HUVECs model, enhanced ICAM-1expression and increased phosphorylation levels of Akt and eNOS were detected in the presence of CRT. Increased phosphorylated eNOS was significantly inhibited by a PI3K inhibitor LY294002 and elevated ICAM-1expression was partially blocked by the inhibitors of both PI3K and eNOS (L-NAME). It has been certified that the RNA-binding protein TTP targets AU-rich elements in the ICAM-1 3′-UTR and suppresses ICAM-1 expression. Knocking down TTP in HUVECs led to an increased induction of ICAM-1 by CRT. We have currently known that activation of p38 downstream kinase MK-2 leads to phosphorylation and inactivation of human TTP. The block of p38 MAPK/MK-2 signaling led to decreased protein expression and mRNA stability of TTP and ICAM-1. Furthermore, L-NAME and/or LY294002 pre-treated HUVECs manifested decreased p38 and MK-2 phosphorylation, which was accompanied by reduced TTP and ICAM-1 protein expression as well as decreased mRNA stability. Our results suggested that CRT could promote ICAM-1 expression in endothelial cells through PI3K/Akt/eNOS/p38 MAPK signaling mediated TTP accumulation, probably in an inactive form, which may provide a possible proinflammatory mechanism of CRT in RA.

1. Introduction

Rheumatoid arthritis (RA) induced synovial inflammation is pathologically characterized by local infiltration of inflammatory cells, which is essential for initiation and perpetuation of inflammatory processes. The main mechanism of the chemotaxis process is inflammatory cells transendothelial migration (TEM). Intercellular adhesion molecule-1 (ICAM-1) and vascular cell adhesion molecule-1 (VCAM-1) play a vital role in leukocyte-endothelial cell interaction which was suggested to facilitate immune responses (Bharadwaj et al., 2016; Yang et al., 2012).

ICAM-1 and VCAM-1 are involved in multiple mechanisms of inflammation progress, predominantly in the performance of local infiltration of inflammatory cells. Actually, ICAM-1 (along with VCAM-1) has been identified as the most important adhesion molecule for TEM (Hua, 2013). Generally, upon triggered by chemokines and cytokines released by endothelium, ICAM-1 and VCAM-1 interact with leukocyte integrins, which lead to the leukocytes arrest during rolling of TEM process (Timmerman et al., 2016). Moreover, ensuing crawling of leukocytes on the vessel wall involves macrophage-1 antigen (Mac-1) binding to ligand ICAM-1 (Lim and Hotchin, 2012). Therefore, ICAM-1 and VCAM-1 are bound to play a key role in the inflammatory reactions

* Corresponding author at: Department of Clinical Immunology, School of Medical Laboratory, Tianjin Medical University, Tianjin 300203, China.
** Corresponding author at: Department of Health Statistics, College of Public Health, Tianjin Medical University, Tianjin 300070, China.
E-mail addresses: majun@tmu.edu.cn (J. Ma), fangzheng@tmu.edu.cn (F. Zheng).
[1] Equal contributors.

https://doi.org/10.1016/j.molimm.2019.01.005
Received 17 June 2018; Received in revised form 2 January 2019; Accepted 4 January 2019
Available online 09 January 2019

of RA infiltrated synovium. Many other potential roles of ICAM-1 and VCAM-1 in the pathogenesis of inflammatory joint disease include T and B lymphocyte activation, angiogenesis and aggressiveness of pannus (Carter and Wicks, 2001). Meanwhile, high levels of soluble ICAM-1 (sICAM-1) and soluble VCAM-1(sVCAM-1) were detected in serum and synovial fluid of patients with early RA (Klimiuk et al., 2007a,b), which was reported to be associated with the autoimmune and inflammatory reactions of RA (Wang et al., 2015).

Regulation of ICAM-1 expression appears to involve both transcriptional and post-transcriptional mechanisms. Transcription factors of ICAM-1 gene such as signal transduction activated transcription factor (STAT), nuclear factor-κB (NF-κB) and activator protein 1(AP-1) are activated by several intracellular signals, particularly PI3K/Akt (Wang et al., 2016; Hou et al., 2014; Tsoyi et al., 2010) signaling pathway in inflammatory microenvironment. The mRNA-binding protein tristetraprolin (TTP) is a key post-transcriptional regulator of ICAM-1 (Shi et al., 2012). TTP suppresses the translation and promotes decay of ICAM-1 mRNA by binding to adenosine/uridine rich elements (AREs) in the 3′-untranslated regions (UTR) of mRNA and then by recruiting deadenylases which shorten the poly (A) tail (Brooks and Blackshear, 2013). Meanwhile, TTP mRNA contains AREs in its own 3′-UTR, which enables a self-negative regulation (Brooks et al., 2004; Tchen et al., 2004). Expression of TTP protein is significantly elevated in synovial tissue of patients with RA (Ross et al., 2017). In addition, knockout of the mouse TTP gene (*Zfp36*) leads to erosive arthritis that is similar to RA (Taylor et al., 1996). The regulation of TTP is closely connected to p38 MAPK signaling pathway. Activation of MAPK-activated protein kinase 2 (MK-2), a p38 MAPK downstream kinase, leads to TTP phosphorylation which further inhibits its ability of degrading target mRNAs (Chrestensen et al., 2004). Therefore, phosphorylated TTP, or inactivated TTP, causes an increased expression of the protein derived from target mRNA.

CRT is an endoplasmic reticulum (ER) resident protein critical for maintaining Ca^{2+} homeostasis and glycoprotein folding in the ER. Extracellular CRT, a member of damage associated molecular patterns (DAMPs), was found to be present at higher concentrations in the plasma and synovial fluid of RA patients and played a role in inhibiting apoptosis of inflammatory T cells in RA (Tarr et al., 2010). Our previous study showed that serum CRT levels were closely related to RA disease activity score (DAS28) (Ni et al., 2013). The pathogenic effect of CRT in RA is associated with nitric oxide (NO) and endothelial nitric oxide synthase (eNOS). eNOS is a critical signaling molecule involved in the regulation of inflammation properties of endothelium. In our earlier study, we demonstrated that extracellular CRT promoted angiogenesis in RA via activation of eNOS (Ding et al., 2014). In addition, CRT was shown to combine with RA shared epitope (SE) that is closely associated with the severity of RA and act as a ligand inducing NO production in opposite cells with resultant immune dysregulation (Holoshitz and Ling, 2007). Furthermore, CRT was found to affect many adhesion-related functions, such as the focal contact initiation, stabilization, turnover (Villagomez et al., 2009) and mediated cell-substratum adhesion (Czarnowski et al., 2014). CRT was involved in the up-regulation of tumor endothelial adhesion molecules and the enhanced infiltration of lymphocytes (Wang et al., 2012). Therefore, the mechanisms of CRT involvement in RA inflammation require further investigation.

Increased understanding of the mechanisms by which CRT exerts its proinflammatory effects in RA will create opportunities for the development of anti-inflammatory therapeutic strategies. The aim of the present study was to investigate the possible molecular mechanism by which CRT participates in RA synovitis inflammation.

2. Materials and methods

2.1. Patients and samples

Serum samples were obtained from patients with RA. Samples of synovial fluid (SF) and synovial membrane (SM) tissues were obtained from patients with RA and OA during synovectomy at Tianjin Medical University General Hospital, Tianjin, China. Patients who suffered from other chronic diseases or any acute infections within 3 months were excluded from this study. All patients with RA fulfilled the American College of Rheumatology and European League Against Rheumatism (ACR/EULAR) 2010 criteria for RA (Sokolove and Strand, 2010) and all patients with OA fulfilled the ACR 1995 criteria for OA (Schouten and Valkenburg, 1995). Local ethics approval for all experiments was provided by the Medical Ethics and Human Clinical Trial Committee of Tianjin Medical University (ethical approval number TMUhMEC 2013031). The informed consent was obtained from all subjects studied.

Serum and SF samples were collected and kept for 1 h at 4 °C, then centrifuged at 1400 *g* for 10 min, and immediately aliquoted and stored at −80 °C. All samples were only allowed to thaw once. SM samples were obtained and placed immediately in sterile RPMI-1640 supplemented with 10% fetal bovine serum (FBS). Paraffin embedded SM were then prepared for immunofluorescence.

2.2. ELISA

The concentration of CRT in serum and synovial fluid were quantified as described previously [26]. Similarly, the expression of ICAM-1 and VCAM-1 in serum and SF were measured by sandwich ELISA kits (Xin Yue Inc., Shanghai, China) according to the manufacturer's protocol. Briefly, Serum and synovial fluid samples were diluted and added to the wells, respectively. The liquid of each well was removed after incubation at 37 °C for 2 h, and 10 μl of biotin-conjugated rabbit anti-human antibodies for indicated proteins were added respectively, followed by incubation for 1 h at 37 °C. After washing, 50 μl of streptavidin-conjugated horseradish peroxidase (HRP) were added and incubated at 37 °C for 1 h followed by addition of chromogenic substrate 3,3′,5,5′- tetramethylbenzidine (TMB). The reaction lasted for 10 min at 37 °C in the dark and was then terminated. The concentrations were assessed by ELISA plate reader at 450 nm.

2.3. ImmunoFluorescence analysis

The expression of CRT, ICAM-1 and VCAM-1 in synovial tissue were detected by immunofluorescence microscopy. Tissue sections (5 μm thick) were cut by a Leica RM2245 paraffin slicer, placed on polylysine-coated glass slides and dried before staining. Tissue sections were then dewaxed in xylene and hydrated through ethanol to water. Slides were rinsed with PBS, fixed with 4% paraformaldehyde for 20 min, permeated with 0.5% triton X-100 for 15 min and blocked with 5% bovine serum albumin (BSA) for 1 h. The primary antibodies to human CRT (MA5-15382; ThermoFisher Scientific, Waltham, MA, USA), ICAM-1 and VCAM-1 (Santa Cruz Biotechnology) were 1:50 diluted and incubated at 37 °C for 1 h in a humidified chamber, respectively. After washing with PBS for three times, the slides were incubated with a FITC conjugated anti-mouse or TRITC conjugated anti-rabbit secondary antibody (ZSGB-BIO, Beijing, China) at 1:250 dilution for 1 h at room temperature. The slides were washed with PBS and counterstained with DAPI for 10 min. The slides were observed using fluorescence microscopy.

2.4. Cell culture and stimulation

A human umbilical vein endothelial cell (HUVEC) culture model was used for in vitro experiments. Primary HUVECs were isolated from fresh human umbilical cords via collagenase digestion, and immediately maintained in DMEM medium supplemented with 10% FBS at 37 °C in an atmosphere of 5% CO_2. All HUVECs were used after no more than five passages. A total of 4×10^5 cells per condition in 2 ml serum free medium was used for stimulation experiments. Cells were

pre-treated for 1 h with 10 μM LY294002 (ProSpec-Tany TechnoGene Ltd.) and/or L-NAME (Santa Cruz Biotechnology, Inc.), or treated for 30 min with 5 μM SB203580 (Selleckchem). Cells were then stimulated with CRT (ProSpec-Tany TechnoGene Ltd.) at the indicated concentration for the indicated time.

2.5. Flow cytometry

The expression of ICAM-1 on HUVECs were detected by flow cytometry. HUVECs in 50–60% confluency were stimulated with recombinant human CRT at various concentrations in the presence or absence of LY294002 or L-NAME in complete DMEM medium. After incubation for 24 h, single cell suspension (contains 1×10^5 to 1×10^6 cells per 100 μl sample) was incubated with FITC-conjugated mouse anti-human antibody for 45 min 4 °C in the dark. After incubation, the cells were washed with PBS buffer for 3 times and resuspended to 500–1000 μl in ice-cold PBS for analysis on flow cytometer.

2.6. Quantitative real-time PCR

Total cellular RNA from HUVECs were extracted using TRIzol (Invitrogen, Carlsbad, CA, USA) and converted to cDNA using Revert Aid TM First Strand cDNA Synthesis Kit (Fermentas, Glen Burnie, MD, USA). Real-time PCR amplification was performed using the platinum SYBR Green qPCR SuperMix-UDG (Invitrogen, Carlsbad, CA, USA), following the manufacturer's instructions. Results were normalized with the ACTB transcript as an internal control and were then used to calculate expression levels according to the ΔΔ comparative threshold method (Pfaffl, 2001). The following primers pairs were used: human ICAM-1 (forward, 5′-CGTGGGGAGAAGGAGCTGAA-3′; reverse, 5′-CAG TGCGGCACGAGAAATTG-3′), human ACTB: forward, 5′−CCCAGGCA CCAGGGCGTGAT-3′; reverse, 5′-TCAAACATGATCTGGGTCAT-3′), TTP: (forward, 5′-ATCCACAACCCTAGCGAAGACCTG-3′; reverse, 5′-ACAGT GGAAGGTCCCCAGGTGGTG-3′).

2.7. Western blot analysis

HUVECs were incubated with various concentrations of CRT in the presence or absence of LY294002 or L-NAME for various time-periods. Proteins were extracted from HUVECs using RIPA lysis buffer supplemented with protease phosphatase inhibitor cocktail (Roche, Mannheim, Germany). Cell lysates were separated by sodium dodecyl sulphate-polyacrylamide gel electrophoresis (SDS-PAGE) and transferred onto polyvinylidene difluoride membranes (Millipore Co., Billerica, MA, USA) at 200 mA for 2 h at 4 °C. The membranes were blocked with 5% BSA (diluted with Tris-buffered saline with 0.1% Tween-20) for 1 h at room temperature and membranes were incubated with primary antibodies overnight at 4 °C. The following antibodies were used: phospho-Akt (Ser473; #4060), Akt (#2920), phospho-eNOS (Ser1177; #9570), eNOS (#32027), phospho-p38 MAPK (Thr180/Tyr182; #4511), p38 MAPK (#9212), phospho-MK-2 (Thr334, #3041), MK-2 (#3042) and β-actin (#3700) (all from Cell Signaling Technology, CA, USA), TTP and ICAM-1 (Abcam). After washing, membranes were incubated with goat anti-rabbit or anti-mouse secondary antibody (ZSGB-BIO, Beijing, China) for 1 h at roomtemperature and proteins were detected using a Pro-light HRP Chemiluminescent Kit (Tiangen Biotech, Beijing, China).

2.8. siRNA-mediated gene silencing

HUVECs were seeded in 12-well plates the day before transfection. Adjust the cell density so that 60 ~ 80% confluency were reached at the time of transfection. Cells were washed with serum-free DMEM, and then incubated with siRNA-containing serum-free media at 37 °C for 24 h before the addition of CRT. siRNA was prepared by mixing Lipofectamine 2000 (1 μl of 1 μg/μl; Invitrogen) and siRNA (25 nM) together in 100 μl of serum-free DMEM, and this mixture was then incubated at room temperature for 30 min. Cells were generally used for assays 24 h post-transfection. siCtr and siTTP were synthesized by RiboBio Co. Ltd (Guangzhou, China). siRNA sequences were: siCtr (UUCUCCGAACGUGUCACGUdTdT), siTTP (CGACGAUAUAAUUAUU AUAdTdT).

2.9. mRNA stability measurement

HUVECs were first pre-treated with SB203580 or L-NAME or LY294002 followed by CRT stimulation as indicated. Then 2 μg/ml of Actinomycin D (Santa Cruz Biotechnology) was added to stop transcription. Cells were lysed for RNA analysis at the indicated times after Actinomycin D addition.

2.10. Statistical analysis

Data were presented as mean ± standard deviation (S.D.) and were processed with SPSS software 16.0. (SPSS Inc., USA). Student's *t*-test was used for a comparison between two different groups. Differences among multi-group were analyzed with one-way analysis of variance (ANOVA), and Student-Newman-Keuls test was further employed for a comparison between two groups. The Pearson product moment correlation coefficient was used for correlation analyses. A P value of less than 0.05 was considered statistically significant.

3. Results

3.1. The levels of CRT in RA serum and synovial fluid correlate positively with ICAM-1 and VCAM-1 levels

Soluble CRT, ICAM-1 and VCAM-1 levels in serum and synovial fluid of patients with RA were determined by ELISA. The correlations were analyzed by Spearman rank correlation coefficients. As shown in Fig. 1A and B, CRT levels were positively correlated with ICAM-1 (R^2 = 0.612, $p < 0.0001$) and VCAM-1 (R^2 = 0.554, $p < 0.0001$), respectively. Then soluble CRT, ICAM-1 and VCAM-1 levels in synovial fluid of patients with RA were also determined. The result showed that CRT levels were positively correlated with ICAM-1 (R^2 = 0.710, p = 0.0031) and VCAM-1 (R^2 = 0.405, p = 0.005), respectively (Fig. 1C and D), which was consistent with the result in serum of RA patients. The demographics and clinical characteristics of patients with RA was shown in Table 1.

3.2. Increased expressions of CRT, ICAM-1 and VCAM-1 in RA synovial tissue

To identify the expression of CRT, ICAM-1 and VCAM-1 in RAST, we performed immunofluorescence on tissue sections. The results showed significantly increased expressions of CRT, ICAM-1 and VCAM-1 in synovial tissue of RA patients compared with those in OA patients (Fig. 2). Strong CRT expression was observed in both lining layer and sublining layer (vascular endothelial cells and perivascular areas) of synovial tissues in RA patients (Fig. 2A and C). Whereas low level of CRT was found in OA tissue sections (Fig. 2B and D). Notably, ICAM-1 was strongly co-expressed with CRT in RA synovium localized to vascular endothelial cells and perivascular areas (Fig. 2A). The co-location of CRT and VCAM-1 was mainly in the lining layer of RA (Fig. 2C).

3.3. Increased ICAM-1expression in HUVECs followed by CRT stimulation

We further identified whether CRT plays a role in the regulation of

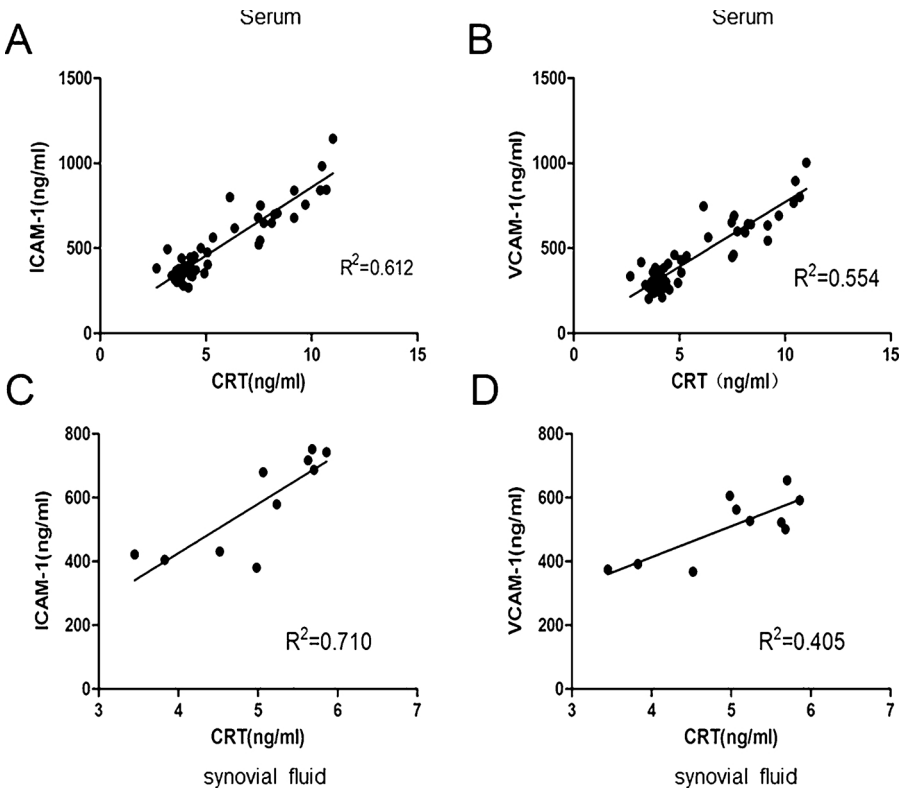

Fig. 1. Correlations between soluble CRT with sICAM-1 and sVCAM-1 in RA patients. CRT, ICAM-1 and VCAM-1 levels in serum (n = 38) and synovial fluid (n = 10) were detected by ELISA. Correlations between CRT with sICAM-1 in **(A)** serum (R^2 = 0.612, $p < 0.001$) and **(C)** synovial fluid (R^2 = 0.710, p = 0.003), and correlations between CRT with sVCAM-1 in **(B)** serum (R^2 = 0.554, $p < 0.001$) and **(D)** synovial fluid (R^2 = 0.405, p = 0.005) were analyzed by Pearson correlation analysis.

Table 1
Demographics and clinical characteristics of patients with Rheumatoid Arthritis (RA).

	Peripheral blood donors	synovial fluid donors
Demographics		
Sex, female/male	25/13	6/4
Age, years*	55 ± 6.52	59 ± 3.16
Disease status		
Disease duration, years*	4.5 ± 5.39	3.0 ± 2.05
DAS28*	4.1 ± 1.55	3.9 ± 0.67
IgM-RF positive (%)	52.6%	70.0%
ACPA positive (%)	13.2%	20.0%
ESR, mm/h*	27.5 ± 4.42	36.0 ± 2.17
CRP, mg/dL*	1.35 ± 0.66	0.79 ± 0.37
Treatment		
Naïve^	0	0
DMARD^	33	9
corticosteroids^	35	7

* Data are expressed as mean ± SD. ^Data are expressed as number. DAS28, disease activity score evaluated in 28 joints; IgM-RF, IgM rheumatoid factor; ACPA, anti-citrullinated protein antibodies; ESR, erythrocyte sedimentation rate; CRP, c-reactive protein; DMARD, disease-modifying anti-rheumatic drugs.

ICAM-1 expression in HUVECs. ICAM-1 expression at protein level on HUVECs stimulated with CRT in different concentrations were determined by flow cytometry (Fig. 3A). It was shown that ICAM-1 expression (represented by MFI) significantly elevated when CRT ≥ 5 ng/ml ($p < 0.01$, Fig. 3b), indicating that CRT incubation consequently led to dose dependent ICAM-1 protein expression (Fig. 3A and B).

Expression of ICAM-1 at mRNA level in HUVECs were explored by real-time PCR. In line with above data, a rising trend of ICAM-1 mRNA levels in HUVECs was observed in the case of 0–50 ng/ml CRT stimulation. A considerable induction of ICAM-1 mRNA expression was caused especially in 10 and 50 ng/ml CRT stimulated cells ($p < 0.01$, Fig. 3C). In summary, our results suggested that CRT promoted ICAM-1 expression in HUVECs at both protein and mRNA levels.

3.4. CRT-induced ICAM-1upregulation is mediated by PI3K/Akt in HUVECs

To address the role of PI3K/Akt signaling pathway in CRT induced ICAM-1 upregulation in HUVECs, we conducted a series of experiments. The effects of CRT on expression and phosphorylation of Akt in HUVECs were examined by western blot. The results showed that elevated phosphorylation levels of Akt in HUVECs were observed with increasing concentrations of CRT stimulation (0, 5, 10, 50 ng/ml). No obvious change of total Akt expression was showed (Fig. 4A). According to these results, a concentration of CRT 10 ng/ml was employed in the following experiments. As expected, continuous exposure to CRT for 0–120 min led to increased Akt phosphorylation in HUVECs. In summary, these data indicated that CRT triggers Akt phosphorylation was in a dose-and time-dependent manner (Fig. 4B).

In order to analyze the impact of PI3K/Akt on the expression of ICAM-1in CRT pretreated HUVECs, a specific PI3K inhibitor LY294002 was used and ICAM-1 expressions were measured by flow cytometry (Fig. 4C). LY294002 treatment partially blocked the effect of CRT on the expression of ICAM-1 in HUVECs ($p < 0.01$, Fig. 4D). These results revealed that CRT stimulation led to ICAM-1 increasing, which was partially inhibited in the presence of PI3K inhibitor (Fig. 4C). Altogether, these findings testified the important role of the induction of PI3K/Akt activation as a determinant of CRT induced ICAM-1 up-regulation.

3.5. CRT induced PI3K/Akt/eNOS signaling mediates ICAM-1 upregulation in HUVECs

To investigate if eNOS is related to CRT induced ICAM-1 upregulation, we measured phosphorylated eNOS in CRT stimulated HUVECs. Interestingly, HUVECs showed a rising trend in eNOS phosphorylation

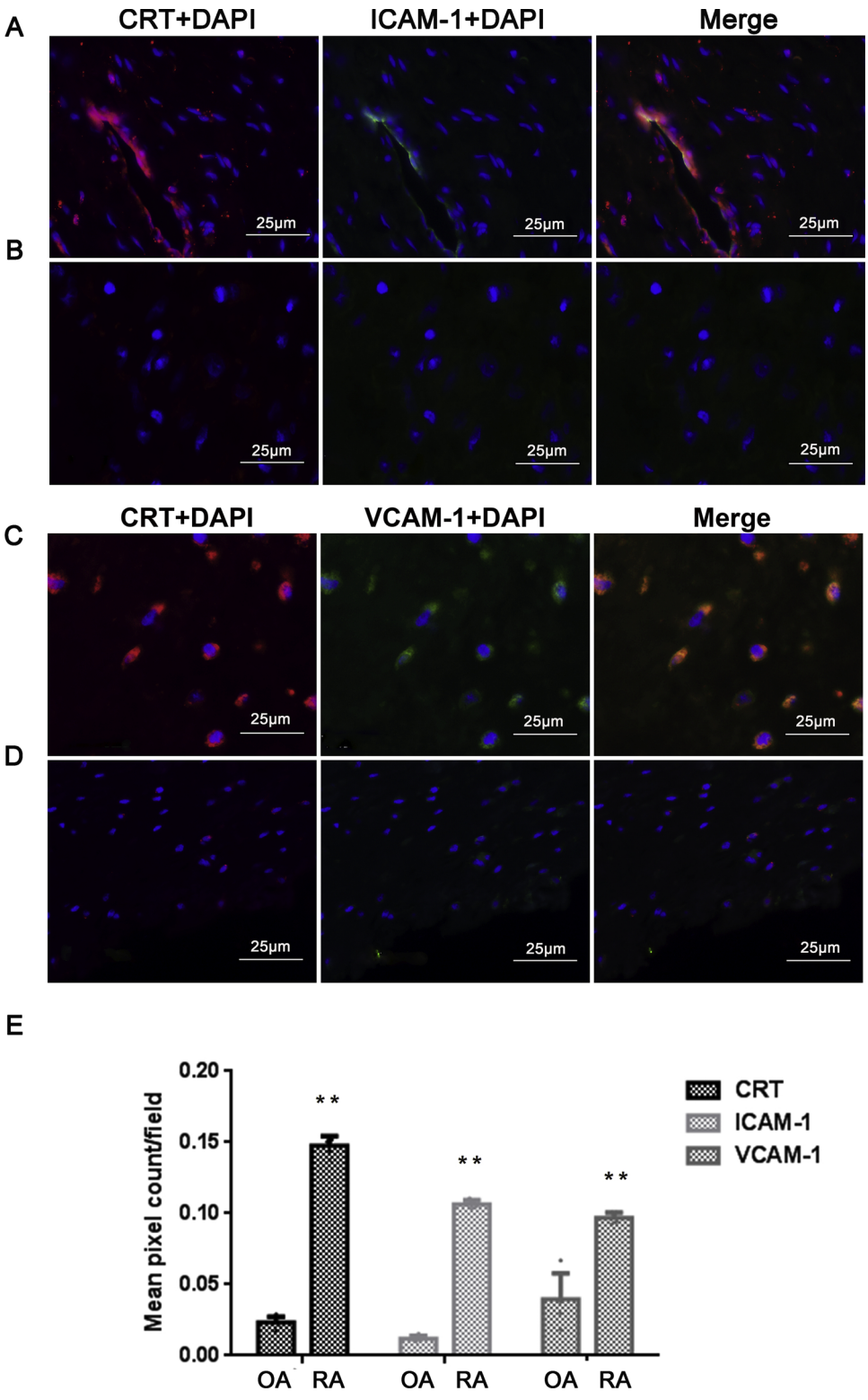

Fig. 2. Increased expressions of CRT, ICAM-1 and VCAM-1 in RA synovial tissue. CRT (red) and ICAM-1 or VCAM-1 (green) in synovial tissue from RA **(A and C)** and OA **(B and D)** were stained, and the slides were observed by fluorescence microscopy. Images are representatives of experiments. **(E)** The staining results of synovial tissues section from OA (n = 4) and RA (n = 4) were quantified using Image *J*, by pixel counting of three fields per section, selected and scanned in blinded manner. Data are shown as mean ± S.D. ** $p < 0.01$ versus OA group (For interpretation of the references to colour in this figure legend, the reader is referred to the web version of this article).

after treated with 0–50 ng/ml CRT (Fig. 5A). Continuous incubation with CRT for 0–120 min also led to elevated eNOS phosphorylation in HUVECs, especially within the range from 30 to 120 min (Fig. 5B). The expression of total eNOS was almost unchanged (Fig. 5A and B). To address the effect of PI3K/Akt on CRT triggered eNOS activation, the specific PI3K inhibitor LY294002 was utilized in CRT (10 ng/ml) stimulated HUVECs. As illustrated, there was an increasing of eNOS phosphorylation with CRT treatment and the impact was partially blocked by LY294002 ($p < 0.01$, Fig. 5C and D). The results showed that CRT partially activated eNOS through PI3K/Akt pathway.

To test if increased phosphorylation of eNOS is involved in the regulation of ICAM-1, we then analyzed ICAM-1 expression in untreated or CRT-treated HUVECs in the presence or absence of an eNOS inhibitor L-NAME (Fig. 5E). Lower ICAM-1 expressions in HUVECs with

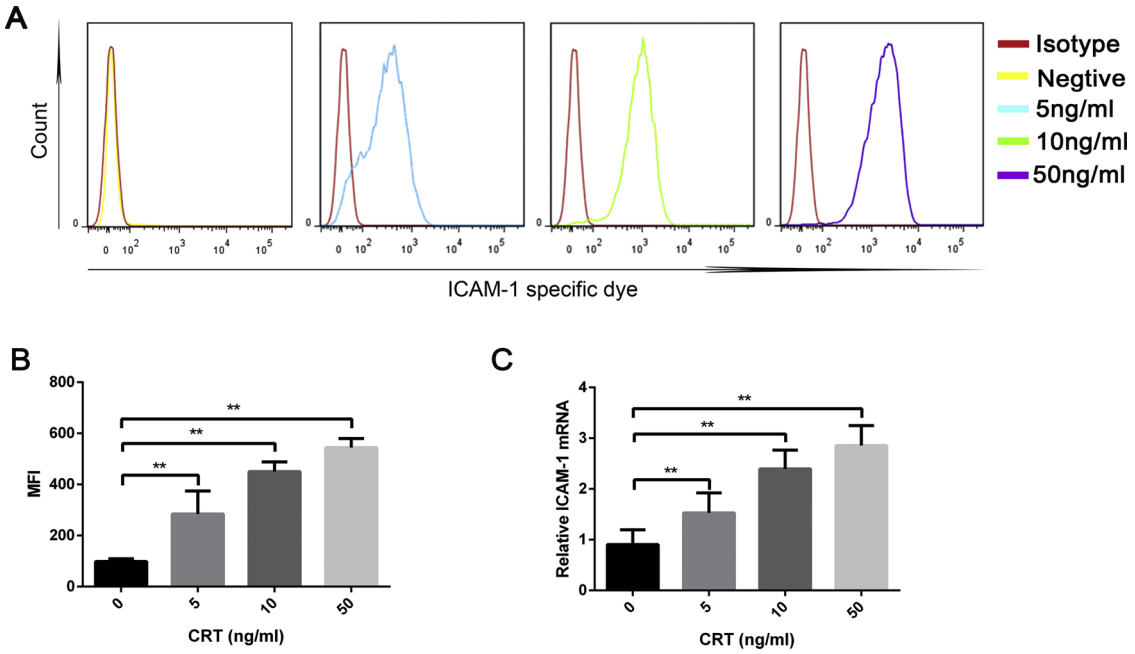

Fig. 3. Increased ICAM-1expression in HUVECs following CRT stimulation. **(A)** HUVECs cultured in the presence of CRT in different concentrations (0, 5, 10, 50 ng/ml) for 12 h were stained for ICAM-1 and analyzed by flow cytometry. The red curve indicates the isotype control. Representative images of three independent experiments are shown. **(B)** Quantification of the above results. The ICAM-1 expression level was depicted as the difference of the mean fluorescent intensity (MFI). ** $p < 0.01$. **(C)** HUVECs cultured in the presence of CRT in different concentrations (0, 5, 10, 50 ng/ml) for 12 h were measured for ICAM-1 mRNA levels by real-time PCR. Indicated ICAM-1 mRNA levels are shown as relative expression normalized to ACTB. ACTB is loading control. ** $p < 0.01$. Data are shown as mean ± S.D. from three independent experiments. (For interpretation of the references to colour in this figure legend, the reader is referred to the web version of this article).

treatment of L-NAME and CRT (10 ng/ml) were exhibited compared with CRT treatment group ($p < 0.01$, Fig. 5E). No significant effect was detected with L-NAME alone. The results revealed that the promoting effects of CRT on ICAM-1were partially inhibited by pre-treatment with L-NAME (Fig. 5F). In summary, it was indicated that PI3K/Akt/eNOS pathway mediated in CRT induced ICAM-1 up-regulation in HUVECs.

3.6. p38 MAPK mediated TTP expression alteration is involved in CRT induced ICAM-1 upregulation

As TTP regulates ICAM-1 expression at the post-transcriptional level, we aimed to test the expression of TTP and the effect of TTP on ICAM-1 expression in response to CRT in this section. To this end we knocked down TTP expression in HUVECs using siRNA and assayed ICAM-1 expression in response to CRT stimulation. TTP expression was

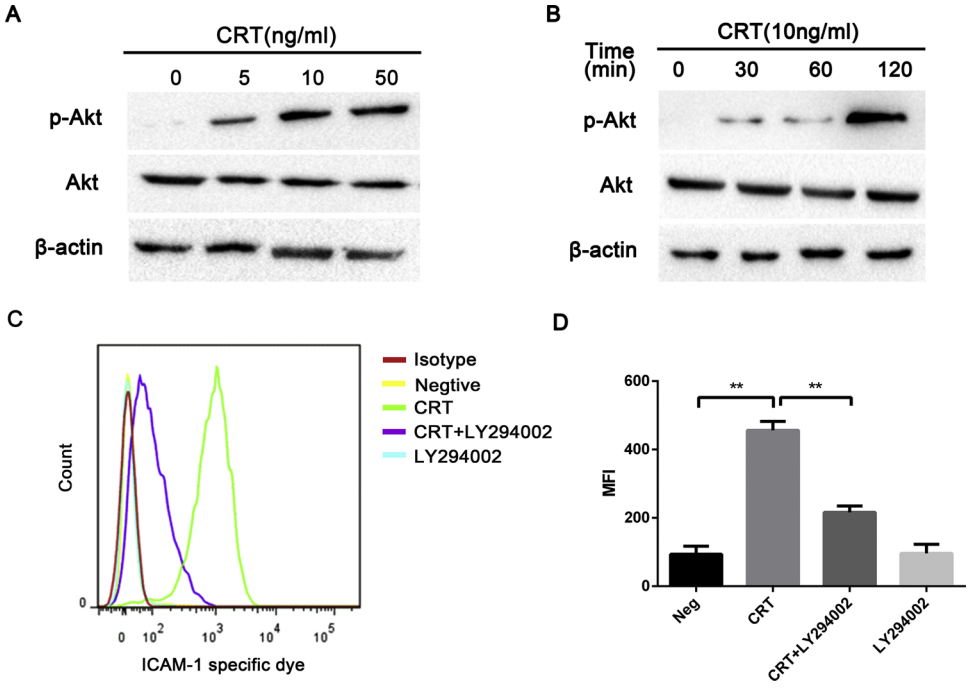

Fig. 4. The effect of PI3K/Akt signaling on CRT-induced ICAM-1upregulation in HUVECs. **(A)** HUVECs were treated with CRT in different concentrations (0, 5, 10, 50 ng/ml) for 2 h, respectively. Total Akt and p-Akt expressions were determined by western blot. **(B)** HUVECs were treated with CRT (10 ng/ml) for 0, 30, 60, 120 min, respectively. Total Akt and p-Akt expressions were determined by western blot. **(A and B)** Representative of three independent experiments. **(C)** HUVECs were pre-incubated for 1 h with LY294002 (10 μM) with or without CRT (10 ng/ml) treatment for 12 h. ICAM-1 expressions in HUVECs were analyzed by flow cytometry. The red curve indicated the isotype control. Representative images of three independent experiments are shown. **(D)** Quantification of **(C)**. ICAM-1 expression was depicted as the difference of MFI. ** $p < 0.01$. Data are shown as mean ± S.D. from three independent experiments. (For interpretation of the references to colour in this figure legend, the reader is referred to the web version of this article).

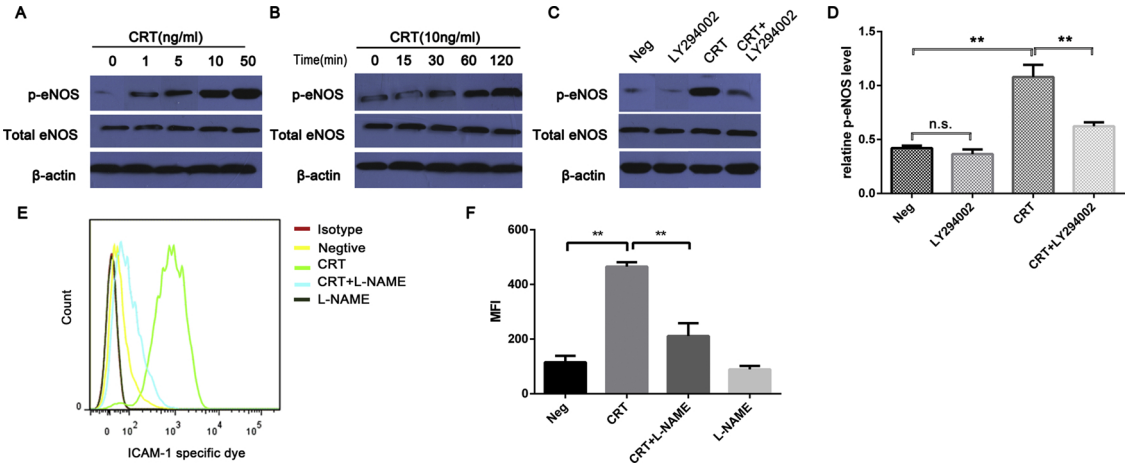

Fig. 5. The effect of PI3K/Akt/eNOS on CRT-induced ICAM-1 upregulation in HUVECs. **(A)** HUVECs were treated with CRT in different concentrations (0, 1, 5, 10, 50 ng/ml) for 2 h, respectively. Total eNOS and p-eNOS expressions were determined by western blot. **(B)** HUVECs were treated with CRT (10 ng/ml) for 0, 15, 30, 60, 120 min, respectively. Total eNOS and p-eNOS expressions were determined by western blot. **(C)** Western Blot analysis of eNOS and p-eNOS in HUVECs treated with 10 μM LY294002 for 1 h followed by CRT (10 ng/ml) for 2 h. **(A, B and C)** Images are representative of three independent experiments. **(D)** Protein abundance in **(C)** was estimated by scanning densitometry, with normalization against the loading control actin. The graph represents mean ± S.D. from three independent experiments. n.s., not significant, ** $p < 0.01$. **(E)** HUVECs treated or not treated with CRT (10 ng/ml) in the presence or absence of L-NAME (10 μM) for 12 h were stained for ICAM-1 and analyzed by flow cytometry. The red curve indicated the isotype control. Representative images of three independent experiments are shown. **(F)** Quantification of **(E)**. The ICAM-1 expression is depicted as the difference of MFI. ** $p < 0.01$. Data are shown as mean ± S.D. from three independent experiments. (For interpretation of the references to colour in this figure legend, the reader is referred to the web version of this article).

efficiently reduced by siRNA transfection, and increased with CRT incubation compared to SiCtr transfection alone (Fig. 6A). Importantly, expression of the known TTP target ICAM-1 was increased in cells lacking TTP expression with CRT treatment (Fig. 6B). In addition, there was a trend to higher ICAM-1 mRNA expression (Fig. 6C), which was consistent with existing research that TTP negatively regulates ICAM-1 expression by facilitating mRNA decay. Given the contradictory result that TTP expression increased with CRT stimulation, we speculated that TTP is accumulated in a phosphorylated and inactive form, which may lead to decreased mRNA decay of itself. Because p38 MAPK is the most extensively studied signaling pathway leading to TTP phosphorylation by MK-2 activation, we wonder if p38 MAPK plays s a role in CRT induced TTP and ICAM-1 expression. Our results revealed that CRT treatment significantly promoted p38 MAPK and MK-2 phosphorylation in a dose-dependent manner (Fig. 6D). To further verification, a p38 MAPK inhibitor SB203580 was used applied. As expected, SB203580 significantly prevented the effect of CRT on the protein expression of TTP (Fig. 6E). The protein expression of ICAM-1 was also decreased by the block of p38 MAPK (Fig. 6E), which was probably a result of increased mRNA decay of ICAM-1 by dephosphorylated TTP. Because AREs are known to destabilize mRNAs (Garneau et al., 2007), we also measured mRNA stabilities of ICAM-1 in HUVECs. We found that ICAM-1 mRNA was more unstable after treatment of SB203580 before CRT compared to CRT treatment alone (Fig. 6F). Notably, TTP mRNA was also destabilized by the p38 MAPK inhibitor, which indirectly supported our hypothesis that upregulated TTP by p38 MAPK may owe to relatively stable mRNA expression. These results showed that CRT induced p38 MAPK activation resulted in increased TTP expression. The increased expression of TTP was probably in a phosphorylation form and therefore led to reduced degradation of mRNA, which maintained the mRNA stability of ICAM-1 as well as itself.

3.7. PI3K/Akt/eNOS signaling promotes the activation of p38 MAPK and facilitates the protein expression and mRNA stability of TTP and ICAM-1 in response to CRT

Since both PI3K/Akt/eNOS and p38 MAPK signaling pathways have a promoting effect on the expression of ICAM-1, we next aimed to figure out if PI3K/Akt/eNOS signaling could affect p38 MAPK activation and TTP expression. Inhibition of eNOS using L-NAME with CRT stimulation led to the declined phosphorylation of p38 and MK-2 (Fig. 7A). Moreover, L-NAME treatment led to reduced expression of TTP and ICAM-1 (Fig. 7A), as expected. The latter result was probably caused by decreased phosphorylation of TTP. Similarly, suppression of PI3K or both PI3K and eNOS resulted in inactivated p38 MAPK /MK-2 signaling as well as decreased TTP and ICAM-1 expression (Fig. 7B and C). After treatment of L-NAME or LY294001 before CRT, the stability of mRNA levels of TTP and ICAM-1 was decreased compared to their basal half-life of ~2 h, but that was enhanced by CRT alone (Fig. 7D). Together, we demonstrated that in the stimulation of CRT, PI3K/Akt/eNOS signaling promoted the activation of p38 MAPK, which further led to the upregulation of TTP and ICAM-1, as well as the mRNA stability of ICAM-1 and TTP itself (Fig. 8).

4. Discussion

RA inflammatory progression is associated with a chronic synovitis. Understanding the molecular mechanisms initiating and perpetuating inflammation in RA is important to define therapeutic strategies (Veale et al., 2017). The present study explored the molecular mechanism of CRT triggered ICAM-1 up-regulation in endothelial cells of RA. We demonstrated that CRT levels in RA were positively correlated with ICAM-1 and VCAM-1, respectively. Subsequent histological observation identified both enhanced co-expressions of CRT with ICAM-1 and VCAM-1 in RA synovial tissues. Further our results manifested an increased ICAM-1 expression in CRT stimulated HUVECs, which could be mediated by PI3K/Akt/eNOS and p38 MAPK signaling pathways. Moreover, the promoting effects of both signalings on ICAM-1 expression were achieved via inhibiting the negative regulation of both protein expression and mRNA stability of ICAM-1 by TTP.

Our results showed that ICAM-1 and VCAM-1 levels in serum of RA patients were positively correlated with CRT, respectively. In our previous studies (Ni et al., 2013), elevated CRT in RA serum had been verified correlated with the degree of RA disease activity. Based on

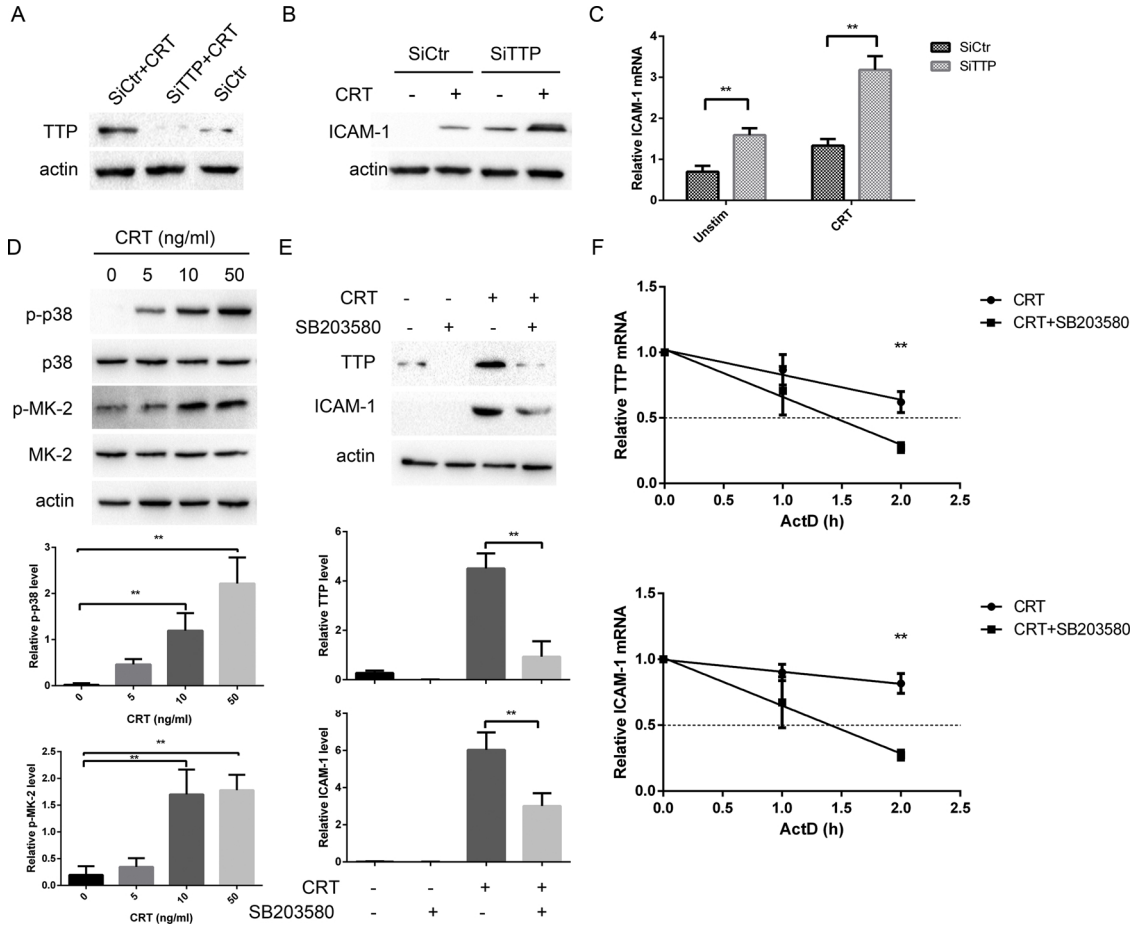

Fig. 6. The enhanced protein expression of TTP by p38 MAPK mediates CRT induced ICAM-1 upregulation. **(A)** HUVECs were transfected with 40 nM control (siCtr) or TTP siRNA (siTTP). Starting from 8 h after transfection, cells were stimulated with 10 ng/ml of CRT for 8 h. TTP and β-actin were analyzed by Western blot. **(B and C)** Cells were transfected as in **(A)**, treated with 10 ng/ml of CRT for 8 h as indicated. ICAM-1 protein and mRNA were measured by western blot and real-time PCR, respectively. **(A and B)** Representative images of three independent experiments are shown. **(C)** Indicated ICAM-1 mRNA levels are shown as relative expression normalized to ACTB. ** $p < 0.01$. Data ae shown as mean ± S.D. from three independent experiments. **(D)** Cells were treated with CRT at 0, 5, 10, 50 ng/ml for 2 h, respectively. Phosphorylated p38, total p38, phosphorylated MK-2 and total MK-2 levels were measured by Western blot. Protein abundance was estimated by scanning densitometry, with normalization against the loading control actin. ** $p < 0.01$. The graph represents mean ± S.D. from three independent experiments. **(E)** Cells were pre-treated with 5 μM SB203580 for 30 min and then incubated with or without 10 ng/ml CRT for 8 h. TTP and ICAM-1 expressions were measured by western blot. TTP and ICAM-1 protein abundance were estimated with normalization against the loading control actin. ** $p < 0.01$. The graph represents mean ± S.D. from three independent experiments. **(F)** Cells were treated with SB203580 (5 μM) for 30 min, followed by CRT (10 ng/ml) stimulation for 8 h as indicated. Actinomycin D (ActD) was added and RNA extracted 0, 1, and 2 h after addition. Gene expression was measured by real-time PCR. TTP and ICAM-1 mRNA levels were normalized to the ACTB. ** $p < 0.01$. Mean ± S.D. from three independent experiments is shown.

those results, the alterations of CRT, ICAM-1 and VCAM-1 expressions and their correlations were additionally examined and analyzed. Considering that SF samples gained from local damaged joints are closely related to the pathological state of RA, relationships between CRT and adhesion molecules were next explored in SF of patients with RA. Similarly, ICAM-1 and VCAM-1 were also positively correlated with CRT in synovial fluid, respectively. Therefore, we speculated that high levels of CRT and highly correlated ICAM-1 and VCAM-1 in RA serum and SF may result from a high local production of those in the inflamed synovium.

In line with these results, obviously elevated expressions of CRT, ICAM-1 and VCAM-1 in synovial tissue of RA patients were observed. Notably, both ICAM-1 and VCAM-1 co-expressed with CRT respectively in RA synovial tissues, yet their distributions were different. ICAM-1 was strongly co-located with CRT in vascular endothelial cells and perivascular areas, and the co-expression of VCAM-1 and CRT was dominantly located in the lining layer. Our results suggested that CRT is involved in cell adhesion molecules mediated inflammatory pathogenesis of RA. ICAM-1 and VCAM-1 up-regulation enables increased immune cell infiltration in the inflamed synovium through TEM process. Moreover, it was reported that high level of soluble ICAM-1 in RA serum was associated with rheumatoid factor (RF), erythrocyte sedimentation rate (ESR) and joint damage (Xu et al., 2014; Klimiuk et al., 2007a,b). ICAM-1 expression is increased by several proinflammatory cytokines and chemokines, including IL-1, IL-6, IL-8, TNF-α and IFN-γ, and by DAMPs (such as HSP70) (Mathur et al., 2011) as well. The present study provided the probability that soluble CRT, regarded as one of the most potent DAMPs, may serve as a pro-inflammatory signal in RA synovitis by contributing to high expression of ICAM-1. All above implied a pathogenic role for CRT in driving the proinflammatory events in RA, and the mechanism might be pertinent to regulation of ICAM-1 and VCAM-1.

For further testification, an *in vitro* cell model, HUVECs, was applied in the subsequent studies. The advantages of using HUVECs are as follows. Firstly, HUVECs could better mimic the status of new vessels in inflammatory microenvironment *in vitro*. Moreover, HUVECs model was employed by most studies in inflammatory mechanism of RA as well, which makes our results more comparable. Our results indicated

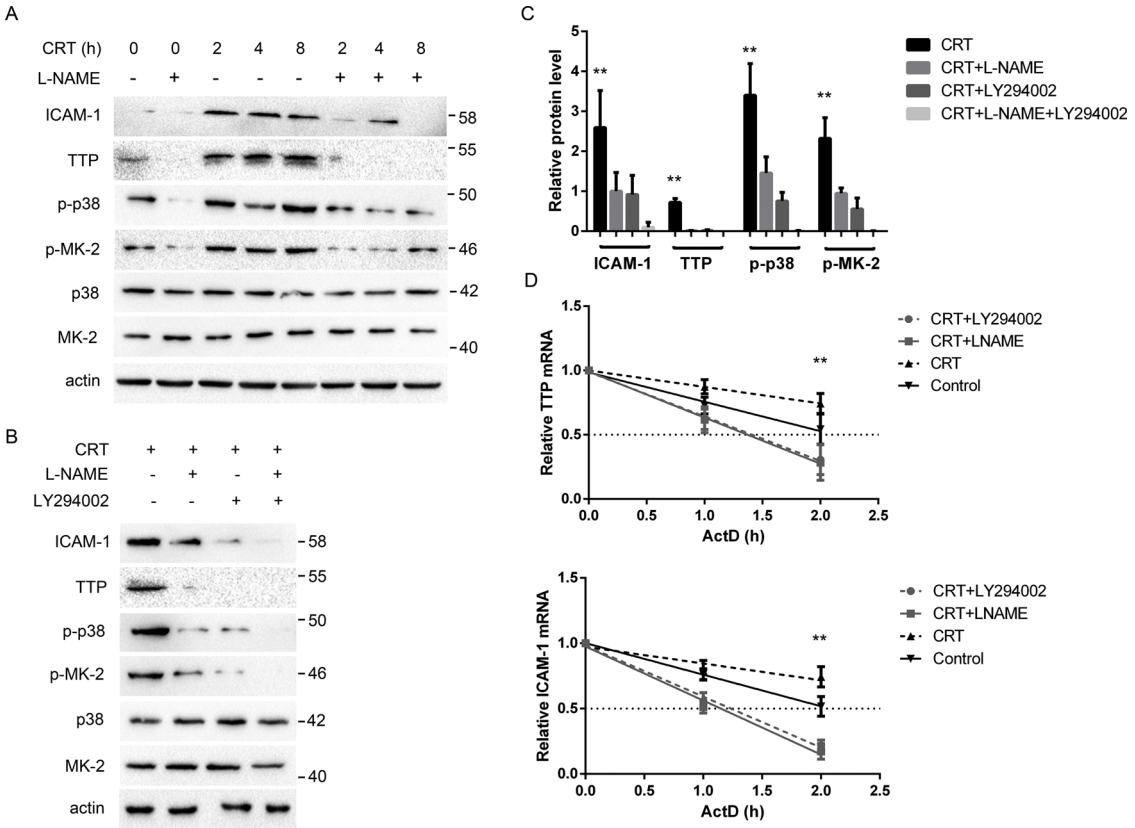

Fig. 7. The effect of PI3K/Akt/eNOS signaling on the activation of p38 MAPK and the expression and mRNA stability of TTP and ICAM-1. **(A)** HUVECs were pre-treated with 10 μM L-NAME for 1 h, followed by 10 ng/ml CRT as indicated. TTP, p-p38, p-MK-2, p38, MK-2, ICAM-1 and β-actin were analyzed by western blot. **(B)** Cells were pre-treated with 10 μM L-NAME and 10 μM LY294002 for 1 h, followed by 10 ng/ml CRT for 8 h as indicated. TTP, p-p38, p-MK-2, p38, MK-2, ICAM-1 and β-actin were analyzed by western blot. **(A and B)** Representative images of at least two independent experiments are shown. **(C)** Protein abundance in **(B)** were estimated by scanning densitometry, with normalization against the loading control actin. ** $p < 0.01$ versus adding inhibitor groups. The graph represents mean ± S.D. from three independent experiments. **(D)** Cells were treated with LY294002 (10 μM) or L-NAME (10 μM) for 1 h, followed by CRT (10 ng/ml) stimulation for 8 h as indicated. Actinomycin D (ActD) was added and RNA extracted 0, 1, and 2 h after addition. Gene expression was measured by real-time PCR. TTP and ICAM-1 mRNA levels were normalized to ACTB. ** $p < 0.01$ CRT group versus adding inhibitor groups. Mean ± S.D. from three independent experiments is shown.

that CRT promoted ICAM-1 expression in HUVECs at both protein and mRNA levels, consistent with a recent study which showed CRT enhanced the expression of both ICAM-1 and VCAM-1 on tumor endothelial cell line resulting in enhanced leukocyte-endothelial cell interactions (Wang et al., 2012). We have demonstrated that CRT may be involved in RA inflammation via contributing to angiogenesis process (Ding et al., 2014). Here, we further defined CRT as an important regulator of ICAM-1expression hallmarking RA inflammation in endothelial cells. Overall the increased transport capability and the enhanced interactive affinity between leukocytes and endothelial cells allowed the efficient entry of circulating immune cells in RA, which at least partially owe to increased CRT level in microenvironment. Consequently, the potential molecular mechanisms involved in the regulation of ICAM-1 by CRT were identified. Several signaling pathways affect ICAM-1 expression favoring the interaction between inflammatory cells and vascular endothelium (Hansson and Edfeldt, 2005). For instance, p38 MAPK signal was suggested to be required in the regulation of ICAM-1 expression caused by LPS, TNF-α (Xiong et al., 2015), Hypochlorite-modified albumin (HOCl-alb) (Tang et al., 2016), IL-1β and Angiotensin II (Liang et al., 2015). PI3K/Akt was also involved in the up-regulation of ICAM-1 induced by pro-inflammatory cytokines TNF-α (Tsoyi et al., 2010) and TGF-α (Hou et al., 2014). At this point, we certified that both PI3K/Akt and p38 MAPK pathways could be activated by CRT, and the former was further capable of phosphorylating eNOS. In addition, our results revealed a cross-talk between PI3K/Akt and p38 MAPK signaling in the regulation of adhesion molecule ICAM-1, that PI3K/Akt/eNOS pathway is an upstream activation signal of p38 MAPK. However, the precise mechanism remains to be explored. Finally, PI3K/Akt/eNOS/p38 MAPK signaling pathway was able to regulate ICAM-1 expression through affecting the expression of TTP, which provided new evidence for the role of CRT in inflammatory diseases.

We demonstrated that TTP could down-regulate ICAM-1 protein and mRNA levels in response to CRT, since siRNA-mediated TTP knockdown led to increased ICAM-1 expression in CRT-stimulated cells. Inconsequently, the expression of TTP was increased by CRT activated PI3K/Akt/eNOS and p38 MAPK signaling pathways, since inhibition of PI3K, eNOS and p38 MAPK led to reduced TTP expression. A likely explanation is that the activation of p38 MAPK by CRT leads to the accumulation of TTP in a phosphorylated and inactive form. Therefore, the mRNA levels of ICAM-1 and other targets such as TTP itself were relatively stable at this stage. Our results are consistent with previously studies to a certain extent (Ngoc et al., 2014; Clement et al., 2011).

In the present study, our results showed a positive correlation of CRT with sICAM-1 and sVCAM-1 in RA, and CRT could upregulate ICAM-1 expression in endothelial cells via PI3K/Akt/eNOS/p38 MAPK signaling pathways mediated TTP expression alteration. In conclusion our investigation revealed further evidence for supporting a pathogenic role of CRT in RA synovitis, providing potential targets for clinical treatment.

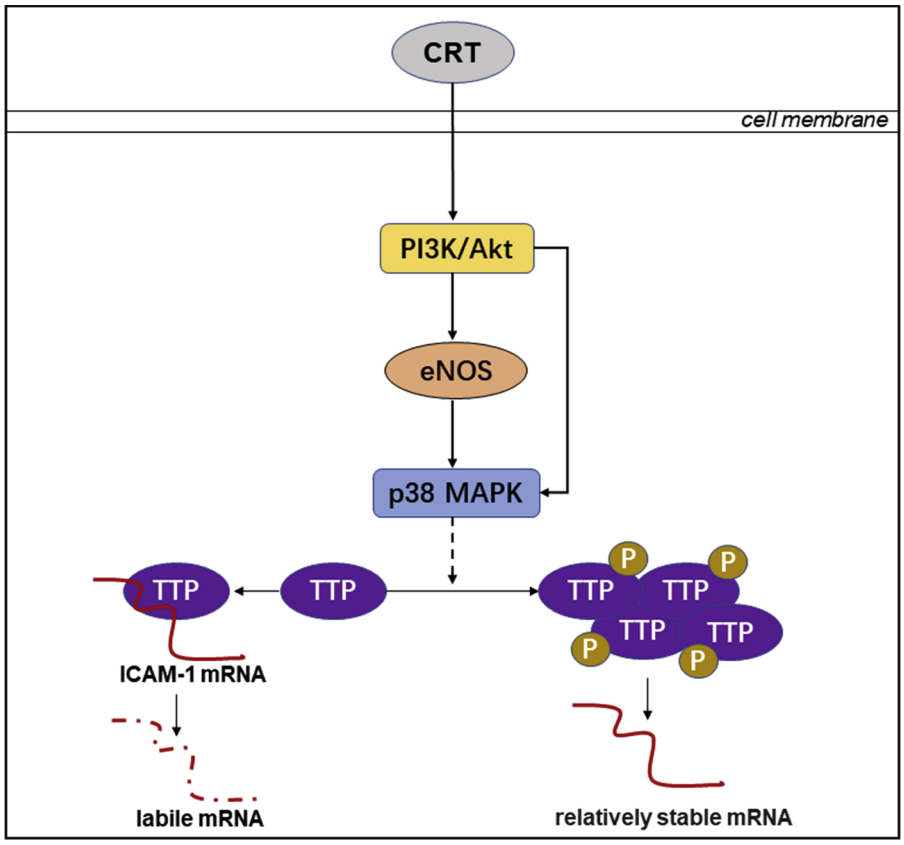

Fig. 8. Signaling pathways involved in CRT-dependent ICAM-1 induction. We hypothesize that CRT stimulation of HUVECs triggers the sequential activation of PI3K/Akt/eNOS and p38 MAPK converging in the increased TTP expression (probably as inactive accumulation of TTP), which leads to increased protein expression as well as mRNA stability of ICAM-1.

Conflicts of interests

The authors declare that they have no conflicts of interest concerning this article.

Acknowledgements

The authors thank Dr. Chunyou Wan (Center for arthrosis, the Hospital of Tianjin) and all the subjects for their assistance in this study.

This study was supported by the Natural Science Foundation of Tianjin City (No. 14JCYBJC25600).

Appendix A. Supplementary data

Supplementary material related to this article can be found, in the online version, at doi:https://doi.org/10.1016/j.molimm.2019.01.005.

References

Bharadwaj, A.S., Stempel, A.J., Olivas, A., Franzese, S.E., Ashander, L.M., Ma, Y., Appukuttan, B., Smith, J.R., 2016. Molecular signals involved in human B cell migration into the retina: in vitro investigation of ICAM-1, VCAM-1, and CXCL13. Ocul. Immunol. Inflamm. 5, 1–9.

Brooks, S.A., Blackshear, P.J., 2013. Tristetraprolin (TTP): interactions with mRNA and proteins, and current thoughts on mechanisms of action. Biochim. Biophys. Acta 1829 (6-7), 666–679.

Brooks, S.A., Connolly, J.E., Rigby, W.F., 2004. The role of mRNA turnover in the regulation of tristetraprolin expression: evidence for an extracellular signal-regulated kinase-specific, AU-Rich element-dependent, autoregulatory pathway. J. Immunol. 172 (12), 7263–7271.

Carter, R.A., Wicks, I.P., 2001. Vascular cell adhesion molecule 1 (CD106): a multifaceted regulator of joint inflammation. Arthritis Rheum. 44 (5), 985–994.

Chrestensen, C.A., Schroeder, M.J., Shabanowitz, J., Hunt, D.F., Pelo, J.W., Worthington, M.T., Sturgill, T.W., 2004. MAPKAP kinase 2 phosphorylates tristetraprolin on in vivo sites including Ser178, a site required for 14-3-3 binding. J. Biol. Chem. 279 (11), 10176–10184.

Clement, S.L., Scheckel, C., Stoecklin, G., Lykke-Andersen, J., 2011. Phosphorylation of tristetraprolin by MK2 impairs AU-rich element mRNA decay by preventing deadenylase recruitment. Mol. Cell. Biol. 31 (2), 256–266.

Czarnowski, A., Papp, S., Szaraz, P., Opas, M., 2014. Calreticulin affects cell adhesiveness through differential phosphorylation of insulin receptor substrate-1. Cell. Mol. Biol. Lett. 19 (1), 77–97.

Ding, H., Hong, C., Wang, Y., Liu, J., Zhang, N., Shen, C., Wei, W., Zheng, F., 2014. Calreticulin promotes angiogenesis via activating nitric oxide signalling pathway in rheumatoid arthritis. Clin. Exp. Immunol. 178 (2), 236–244.

Garneau, N.L., Wilusz, J., Wilusz, C.J., 2007. The highways and byways of mRNA decay. Nat. Rev. Mol. Cell Biol. 8 (2), 113–126.

Hansson, G.K., Edfeldt, K., 2005. Toll to be paid at the gateway to the vessel wall. Arterioscler. Thromb. Vasc. Biol. 25 (6), 1085–1087.

Holoshitz, J., Ling, S., 2007. Nitric oxide signaling triggered by the rheumatoid arthritis shared epitope: a new paradigm for MHC disease association? Ann. N. Y. Acad. Sci. 1110, 73–83.

Hou, C.H., Lin, F.L., Tong, K.B., Hou, S.M., Liu, J.F., 2014. Transforming growth factor alpha promotes osteosarcoma metastasis by ICAM-1 and PI3K/Akt signaling pathway. Biochem. Pharmacol. 89 (4), 453–463.

Hua, S., 2013. Targeting sites of inflammation: intercellular adhesion molecule-1 as a target for novel inflammatory therapies. Front. Pharmacol. 4, 127.

Klimiuk, P.A., Fiedorczyk, M., Sierakowski, S., Chwiecko, J., 2007a. Soluble cell adhesion molecules (sICAM-1, sVCAM-1, and sE-selectin) in patients with early rheumatoid arthritis. Scand. J. Rheumatol. 36 (5), 345–350.

Klimiuk, P.A., Fiedorczyk, M., Sierakowski, S., Chwiecko, J., 2007b. Soluble intercellular adhesion molecule-1 (ICAM-1) antigen in patients with rheumatoid arthritis. Scand. J. Rheumatol. 36 (5), 345–350.

Liang, B., Wang, X., Zhang, N., Yang, H., Bai, R., Liu, M., Bian, Y., Xiao, C., Yang, Z., 2015. Angiotensin-(1-7) attenuates angiotensin II-Induced ICAM-1, VCAM-1, and MCP-1 expression via the MAS receptor through suppression of P38 and NF-κB pathways in HUVECs. Cell. Physiol. Biochem. 35 (6), 2472–2482.

Lim, J., Hotchin, N.A., 2012. Signalling mechanisms of the leukocyte integrin αMβ2: current and future perspectives. Biol. Cell 104 (11), 631–640.

Mathur, S., Walley, K.R., Wang, Y., Indrambarya, T., Boyd, J.H., 2011. Extracellular heat shock protein 70 induces cardiomyocyte inflammation and contractile dysfunction via TLR2. Circ. J. 75 (10), 2445–2452.

Ngoc, L.V., Wauquier, C., Soin, R., Bousbata, S., Twyffels, L., Kruys, V., Gueydan, C., 2014. Rapid Proteasomal Degradation of Posttranscriptional Regulators of the TIS11/Tristetraprolin Family Is Induced by an Intrinsically Unstructured Region Independently of Ubiquitination. Mol. Cell. Biol. 34 (23), 4315–4328.

Ni, M., Wei, W., Wang, Y., Zhang, N., Ding, H., Shen, C., Zheng, F., 2013. Serum levels of calreticulin in correlation with disease activity in patients with rheumatoid arthritis. J. Clin. Immunol. 33 (5), 947–953.

Pfaffl, M.W., 2001. A new mathematival model for reletive quantification in real-time RT-PCR. Nucleic Acids Res. 29 (9), e45.

Ross, E.A., Naylor, A.J., O'Neil, J.D., Crowley, T., Ridley, M.L., Crowe, J., Smallie, T.,

Tang, T.J., Turner, J.D., Norling, L.V., Dominguez, S., Perlman, H., Verrills, N.M., Kollias, G., Vitek, M.P., Filer, A., Buckley, C.D., Dean, J.L., Clark, A.R., 2017. Treatment of inflammatory arthritis via targeting of tristetraprolin, a master regulator of pro-inflammatory gene expression. Ann. Rheum. Dis. 76 (3), 612–619.

Schouten, J.S., Valkenburg, H.A., 1995. Classification criteria: methodological considerations and results from a 12 year following study in the general population. J. Rheumatol. Suppl. 43, 44–45.

Shi, J.X., Su, X., Xu, J., Zhang, W.Y., Shi, Y., 2012. MK2 posttranscriptionally regulates TNF-α-induced expression of ICAM-1 and IL-8 via tristetraprolin in human pulmonary microvascular endothelial cells. Am. J. Physiol. Lung Cell Mol. Physiol. 302 (8), L793–9.

Sokolove, J., Strand, V., 2010. Rheumatoid arthritis classification criteria - it's finally time to move on! Bull. NYU Hosp. Jt. Dis. 68 (3), 232–238.

Tang, D.D., Niu, H.X., Peng, F.F., Long, H.B., Liu, Z.R., Zhao, H., Chen, Y.H., 2016. Hypochlorite-modified albumin upregulates ICAM-1 expression via a MAPK-NF-κB signaling cascade: protective effects of Apocynin. Oxid. Med. Cell. Longev. 2016, 1852340.

Tarr, J.M., Winyard, P.G., Ryan, B., Harries, L.W., Haigh, R., Viner, N., Eggleton, P., 2010. Extracellular calreticulin is present in the joints of patients with rheumatoid arthritis and inhibits FasL (CD95L)-mediated apoptosis of T cells. Arthritis Rheum. 62 (10), 2919–2929.

Taylor, G.A., Carballo, E., Lee, D.M., Lai, W.S., Thompson, M.J., Patel, D.D., Schenkman, D.I., Gilkeson, G.S., Broxmeyer, H.E., Haynes, B.F., Blackshear, P.J., 1996. A pathogenetic role for TNFa in the syndrome of Cachexia, arthritis, and autoimmunity resulting from tristetraprolin (TTP) deficiency. Immunity 4 (5), 445–454.

Tchen, C.R., Brook, M., Saklatvala, J., Clark, A.R., 2004. The stability of tristetraprolin mRNA is regulated by mitogen-activated protein kinase p38 and by tristetraprolin itself. J. Biol. Chem. 279 (31), 32393–32400.

Timmerman, I., Daniel, A.E., Kroon, J., van Buul, J.D., 2016. Leukocytes crossing the endothelium: a matter of communication. Int. Rev. Cell Mol. Biol. 322, 281–329.

Tsoyi, K., Jang, H.J., Nizamutdinova, I.T., Park, K., Kim, Y.M., Kim, H.J., Seo, H.G., Lee, J.H., Chang, K.C., 2010. PTEN differentially regulates expressions of ICAM-1 and VCAM-1 through PI3K/Akt/GSK-3beta/GATA-6 signaling pathways in TNF-alpha-activated human endothelial cells. Atherosclerosis 213 (1), 115–121.

Veale, D.J., Orr, C., Fearon, U., 2017. Cellular and molecular perspectives in rheumatoid arthritis. Semin. Immunopathol. 39 (4), 343–354.

Villagomez, M., Szabo, E., Podcheko, A., Feng, T., Papp, S., Opas, M., 2009. Calreticulin and focal-contact-dependent adhesion. Biochem. Cell Biol. 87 (4), 545–556.

Wang, H.T., Lee, H.I., Guo, J.H., Chen, S.H., Liao, Z.K., Huang, K.W., Torng, P.L., Hwang, L.H., 2012. Calreticulin promotes tumor lymphocyte infiltration and enhances the antitumor effects of immunotherapy by up-regulating the endothelial expression of adhesion molecules. Int. J. Cancer 130 (12), 2892–2902.

Wang, L., Ding, Y., Guo, X., Zhao, Q., 2015. Role and mechanism of vascular cell adhesion molecule-1 in the development of rheumatoid arthritis. Exp. Ther. Med. 10 (3), 1229–1233.

Wang, Y., Cao, J., Fan, Y., Xie, Y., Xu, Z., Yin, Z., Gao, L., Wang, C., 2016. Artemisinin inhibits monocyte adhesion to HUVECs through the NF-kappaB and MAPK pathways in vitro. Int. J. Mol. Med. 37 (6), 1567–1575.

Xiong, H., Xu, Y., Tan, G., Han, Y., Tang, Z., Xu, W., Zeng, F., Guo, Q., 2015. Glycyrrhizin ameliorates imiquimod-induced psoriasis-like skin lesions in BALB/c mice and inhibits TNF-α-induced ICAM-1 expression via NF-κB/MAPK in HaCaT cells. Cell. Physiol. Biochem. 35 (4), 1335–1346.

Xu, F.F., Zhu, H., Li, X.M., Yang, F., Chen, J.D., Tang, B., Sun, H.G., Chu, Y.N., Zheng, R.X., Liu, Y.L., Wang, L.S., Zhang, Y., 2014. Intercellular adhesion molecule-1 inhibits osteogenic differentiation of mesenchymal stem cells and impairs bio-scaffold-mediated bone regeneration in vivo. Tissue Eng. A 20 (19–20), 2768–2782.

Yang, J.C., Huang, F., Wu, C.J., Chen, Y.C., Lu, T.H., Hsieh, C.H., 2012. Simvastatin reduces VCAM-1 expression in human umbilical vein endothelial cells exposed to lipopolysaccharide. Inflamm. Res. 61 (5), 485–491.